Class IA Phosphoinositide 3-Kinase Modulates Basal Lymphocyte Motility in the Lymph Node[1]

Melanie P. Matheu,* Jonathan A. Deane,† Ian Parker,*‡ David A. Fruman,[2†§] and Michael D. Cahalan[2,3*§]

Recruitment of PI3K to the cell membrane is an indispensable step in normal lymphocyte proliferation and activation. In this study we identify PI3K as an important signaling molecule for maintaining basal T and B lymphocyte motility and homing in the intact lymph node. Pharmacological inhibition of PI3K catalytic isoforms exerted broad effects on basal lymphocyte motility, including changes in homing kinetics, localization of B cells within the lymph node, and reduced cell velocities. Lymphocytes deficient in either or both of the class IA PI3K regulatory subunits p85α and p85β also exhibited reduced velocities, with the magnitude of reduction depending upon both cell type and isoform specificity. B cells deficient in p85α exhibited gross morphological abnormalities that were not evident in cells treated with a PI3K inhibitor. Our results show, for the first time, that class IA PI3Ks play an important role in regulating basal lymphocyte motility and that p85α regulatory subunit expression is required to maintain B cell morphology in a manner independent of PI3K catalytic function. Moreover, we demonstrate distinct roles for catalytic domain function and class IA PI3K regulatory domain activity in lymphocyte motility, homing, and homeostatic localization of mature resting B cells. *The Journal of Immunology,* **2007, 179: 2261–2269.**

Phosphoinositide 3-kinases constitute a class of lipid kinases that phosphorylate the 3′-hydroxyl of D-*myo*-phosphatidylinositol and its derivatives. Class I PI3Ks phosphorylate phosphatidylinositol-4,5-bisphosphate to produce phosphatidylinositol-3,4,5-trisphosphate (PtdIns(3,4,5)P_3),[4] a critical second messenger in immune responses, lymphocyte development, and survival. Aberrant regulation of class I PI3K signaling is implicated in autoimmunity, leukemia, and lymphoma, whereas reduced activity leads to immunodeficiency (1).

Class I PI3Ks are heterodimers composed of a regulatory subunit and a tightly associated catalytic subunit. Class I PI3Ks are further subdivided into class IA and class IB regulatory and catalytic isoforms. Class IA PI3K is represented by five regulatory subunits encoded by three genes. *Pik3r1* encodes p85α and its alternative transcripts p55α and p50α, *Pik3r2* encodes p85β, and *Pik3r3* encodes p55γ. These regulatory subunits bind tightly to one of the three catalytic isoforms, p110α, p110β, and p110δ, and recruit the complex to the membrane upon receptor ligation and phosphorylation. Class IA PI3Ks are activated downstream of immune cell receptors including the BCR, TCR, costimulatory molecules, and cytokine receptors that are phosphorylated by tyrosine kinases upon cognate stimulus (1). The most abundant regulatory isoforms in T cells are p85α and p50α, with lesser amounts of p85β; B cells express mainly p85α with low levels of p85β and p50α (2, 3).

Class IB PI3K receptors are thought to be involved in chemotactic responses because they are recruited to the membrane upon chemokine receptor activation (4). A single class IB PI3K catalytic isoform (p110γ) can pair with one of two regulatory subunits (p84/p87 or p101) and is activated by G$\beta\gamma$ subunits downstream of G protein-coupled receptors (4). PtdIns(3,4,5)P_3 produced by class IB PI3K contributes to F-actin polymerization through the recruitment of guanine nucleotide exchange factors to the leading edge of neutrophils (4). Neutrophils lacking p110γ and those treated with PI3K inhibitors have decreased motility toward chemoattractants and change direction more frequently (5, 6). PI3K inhibitors also inhibit T cell chemotaxis to various chemokines (4, 7). Furthermore, mice lacking dedicator of cytokinesis 2 (DOCK2) suggested a DOCK2-independent contribution of p110γ in T lymphocyte homing and localization within the lymph node (8). In addition, DOCK2/p110γ double knockout (KO) T lymphocytes do not migrate in vitro to CCL21 (8). However, in a recent study T cell motility in the lymph node was shown to be reduced in DOCK2 KO T cells with no additional effect seen in p110γ (class IB PI3K) null T and B cells (9).

Growing evidence points to an evolutionarily conserved participation of class IA PI3K in cell motility and chemotaxis. Notably, class IA homologues play a role in *Dictyostelium discoideum* motility and chemotaxis in which PI3K lipid products are localized to the leading edge during chemotaxis (10). In Jurkat T cells, expression of a dominant-negative class IA p85α regulatory subunit reduced chemotaxis to stromal cell-derived factor-1 (SDF-1) (11). Moreover, the catalytic isoform p110δ plays a role in B cell chemotaxis to CXCL13 and alters CXCR4 chemokine receptor expression (7). In B lymphocytes, PI3K inhibitors reduce chemotaxis to CXCL13 and DOCK2-independent homing, yet p110γ is not

*Department of Physiology and Biophysics, †Department of Molecular Biology and §Biochemistry, ‡Department Neurobiology and Behavior, and Center for Immunology, University of California, Irvine, California 92697

Received for publication December 19, 2006. Accepted for publication May 31, 2007.

The costs of publication of this article were defrayed in part by the payment of page charges. This article must therefore be hereby marked *advertisement* in accordance with 18 U.S.C. Section 1734 solely to indicate this fact.

[1] This work was supported by National Institutes of Health Grants GM41514 (to M.D.C.), AI50831 (to D.A.F.), and GM-48071 (to I.P.) and by National Institutes of Health Kirchstein Fellowship AI-64128 (to M.P.M.).

[2] D.A.F. and M.D.C. contributed equally to this work.

[3] Address correspondence and reprint requests to Dr. Michael D. Cahalan, Department of Physiology and Biophysics, University of California, Irvine, CA 92697-4561. E-mail address: mcahalan@uci.edu

[4] Abbreviations used in this paper: PtdIns(3,4,5)P_3, phosphatidylinositol-3,4,5-trisposphate; CMTMR, 5-(and-6)-(((4-chloromethyl) benzol) amino)tetramethylrhodamine); DOCK2, dedicator of cytokinesis 2; KO, knockout; SDF-1, stromal cell-derived factor-1; WMN, wortmannin.

required for these responses (6). In addition, class IA PI3K functions upstream and downstream of integrin activation in various cell types, providing a possible mechanism for regulating lymphocyte motility and polarization in the native environment of the lymph node (12–16).

In this study, we used pharmacological and genetic approaches to demonstrate that PI3K catalytic activity and regulatory domain function play distinct roles in regulating basal lymphocyte motility. To assess the involvement of PI3K catalytic subunits in T and B cell motility, homing, and localization we initially used wortmannin (WMN), which is a potent (IC_{50} = 5 nM) and covalent inhibitor of PI3K catalytic domains. Although specific for PI3K inhibition, WMN does not distinguish between class IA and IB PI3K catalytic isoforms (1), and we further investigated the specific role of class IA PI3K in lymphocyte motility by using lymphocytes lacking individual or multiple class IA PI3K regulatory isoforms. Class IA regulatory subunits have adaptor functions that regulate additional cellular processes such as actin polymerization as well as direct the localization and activity of PI3K catalytic subunits (17). Our results demonstrate a specific contribution of different class IA regulatory isoforms to basal T and B lymphocyte motility in the lymph node and a role for the p85α regulatory isoform, but not PI3K catalytic activity, in maintaining B cell morphology in vivo.

Materials and Methods

Two-photon imaging and data analysis

Imaging was performed with a custom-built, two-photon microscope system as described, except that three photomultiplier channels were used for simultaneous imaging of green-, red-, and blue-labeled lymphocytes (18, 19). The system was based on an upright Olympus BX50 microscope fitted with a ×20 water-immersion objective (numerical aperture 0.95), a Spectra-Physics Tsunami femtosecond laser tuned to 780 nm, an *x-y* mirror scan head, and a motorized focus controller (Prior Scientific). Image acquisition operated under software control (METAMORPH; Universal Imaging). Three-dimensional image stacks (*x*, *y*, and *z*) were acquired at time intervals ranging between 26 and 18 s. In situ lymph node imaging was conducted in freshly isolated lymph nodes under a continuous flow of oxygen-perfused RPMI 1640 kept at 37°C as previously described (19). Images and videos show maximum intensity projections along the *z*-axis, representing a "top" (*x–y*) view of the volume. For three-color B cell experiments, cells were tracked within 10-μm-deep *z*-axis projections; otherwise the imaging volume was 50-μm deep. All results are presented as mean ± 1 SEM. Tests of statistical significance were performed using a two-tailed Student's *t* test.

Adoptive transfer, wortmannin treatment, and cell labeling

$CD4^+$ T cells or $CD43^-$ B cells were purified from C57BL/6 donor animals using magnetic bead separation (Miltenyi Biotec). Half of the purified lymphocytes were labeled with the cell tracker dye 5-(and 6)-(((4-chloromethyl)benzol)amino)tetramethylrhodamine (CMTMR) (red fluorescence; Molecular Probes) and the other half with CFSE (green; Molecular Probes) together with 50 nM WMN for 15 min at 37°C. Labeled lymphocytes were recombined and coinjected via the tail vein into a genetically identical recipient. Lymph nodes in T and B cell recipients were harvested after 2 and 4 h, respectively. Wild-type, untreated CFSE-, and CMTMR-labeled cells were coinjected in experiments to ensure that the velocity data were not label dependent. In three-color B cell experiments, 12–15 million naive B lymphocytes were purified, labeled blue with 4-chloromethyl-6,8-difluoro-7-hydroxycourmarin (Molecular Probes), and injected 3 days before the coinjected WMN-treated and control B cell populations.

Antibodies and flow cytometric analysis

For homing experiments, samples of the recombined, injected cell populations were assessed by FACS to determine the exact proportions of coinjected cells and were later used to normalize FACS data if necessary. In all homing experiments the largest difference accounted for was 10%, which was used to normalize the resultant FACS data of whole tissue homogenate. Blood and spleen lymphocytes were prepared for FACS by water lysis. In FACS analysis, chemokine receptors of the lymphocytes were labeled with anti-CXCR4 clone 2B11/CXCR4 (BD Biosciences), anti-CXCR5 clone 2G8 (BD Biosciences), or anti-CCR7 clone 4B12 (eBioscience).

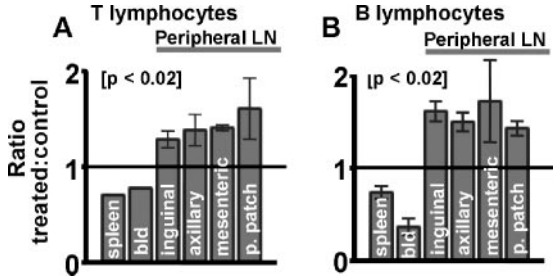

FIGURE 1. Inhibition of the PI3K catalytic subunits alters lymphocyte homing. *A*, This bar graph gives ratios of 50 nM WMN-treated $CD4^+$ T lymphocytes to untreated internal control T lymphocytes present in blood and various lymphoid tissues 2 h following the adoptive transfer of labeled T cells. *B*, Corresponding ratios of 50 nM WMN-treated B lymphocytes to control B lymphocytes obtained 4 h after adoptive transfer. Cell ratios were analyzed by FACS of whole organ homogenates (n = 3). In both cases, the ratios are corrected for small (≤10%) inequalities assessed by FACS in treated vs untreated lymphocytes in the preparations used for adoptive transfer. bld, Blood; LN, lymph node; p. patch, Peyer's patch.

Cytokines and Transwell assays

Cytokines were obtained from R&D Systems and diluted in medium containing 0.5% fatty acid-free BSA. Transwell assay plates with 5-μm pore size were obtained from Neuro Probe. Freshly isolated B or T lymphocytes were treated with either 50, 100, or 250 nM WMN for 15 min and washed twice in 0.5% fatty acid-free BSA-containing medium. The percentage migrated was calculated as a percentage of the total input. Each chemotaxis assay was performed in triplicate for three separate experiments.

Knockout animals

The generation of mice lacking p85α or p85β alone is described elsewhere (2, 3, 20, 21). T lymphocytes lacking p85α and p85β gene products were generated by breeding *Pik3r1*^{f} (p85α-floxed) mice with *Pik3r2*^{n} (p85β-null) mice (2, 3) and Lck-Cre transgenic mice (22). All mice were maintained in a mixed background (C57BL/6 × 129SvEv) and were studied at 2–4 mo of age. Wild-type F_1 C57BL/6 × 129SvEv mice were used as control animals. We found no differences in T cell velocity in adoptively transferred C57BL/6 × 129SvEv cells in littermate recipients, when compared with C57BL/6 transferred into C57BL/6, as late as 8 h after adoptive transfer (data not shown). Animals were housed in autoclaved microisolator cages with sterilized food and water. All procedures were approved by the University of California Irvine Institutional Animal Care and Use Committee.

Results

Inhibition of PI3K catalytic function alters lymphocyte homing

The contribution of PI3K catalytic activity to basal regulation of lymphocyte localization was evaluated by comparing the homing of adoptively transferred control lymphocytes with that of lymphocytes pretreated with the covalent catalytic subunit inhibitor WMN at 50 nM for 15 min. As expected, under these conditions the PI3K signaling output was reduced to background by the measurement of phosphorylated AKT (data not shown). WMN-treated T or B cells were labeled with the cell tracker dye CFSE (green) and coinjected in equal proportions with corresponding control (untreated) lymphocytes labeled with CMTMR (red). Two hours after $CD4^+$ T cell adoptive transfer and 4 h after the transfer of mature resting $CD43^-$ B cells, samples of blood, lymph nodes, and spleen were analyzed by FACS to determine the ratio of WMN-treated and untreated lymphocytes. At these times, the numbers of WMN-treated lymphocytes (both T cells and B cells) were greater relative to those of coinjected internal control cells in peripheral lymph nodes, whereas their relative abundance was correspondingly reduced in the blood and spleen (Fig. 1, *A* and *B*). Similar results were obtained with a higher concentration (100 nM) of

WMN and after switching the CFSE and CMTMR labels (data not shown).

PI3K catalytic inhibition disrupts B cell localization in follicles and reduces B cell velocity

WMN-treated (50 nM) B cells (CFSE, green) were found concentrated in an area distinct from coinjected control B cells (CMTMR, red), as illustrated in supplemental video 1.[5] To examine their distribution in relation to the B cell follicle, we imaged WMN-treated B cells in nodes from mice that had been injected 3 days earlier with counterstained control B cells that served to mark the B cell follicle. Fig. 2*A* shows a representative image from a triple-labeling experiment (supplemental video 2) with 3-day resident B cells in blue and B cells adoptively transferred 4 h before imaging shown in red (controls) and green (WMN-treated). The recently transferred control B cells did not have sufficient time to fully localize and although many were evident within the follicle, others were present at the follicle edge. In contrast, the WMN-treated B cells transferred at the same time were substantially excluded from the follicle and instead were present at high density at the edge of the B cell follicle (Fig. 2*A*). This alteration in B cell localization was reflected by a change in the preferential directional motion of the WMN-treated B cells relative to control B cells. Untreated B cells (both 3-day and 4-h residents) within the center of the follicle demonstrated the random walk motility typical of resting lymphocytes, whereas at the follicle edge both showed a strong directional preference toward the follicle (Fig. 2, *B* and *C*). In marked contrast, the WMN-treated B cells demonstrated near random motility at the follicle edge and tended to move toward the follicle edge when tracked from the center of the follicle (Fig. 2, *B* and *C*).

Measurements of instantaneous B cell velocities revealed that WMN treatment reduced the average velocity by 21% as compared with control cells tracked simultaneously in the same imaging records (5.0 vs 6.2 μm min^{-1}; Fig. 2*D*). The failure of WMN-treated B cells to localize within the follicle after adoptive transfer might result simply from reduced velocity. However, no significant change in regional distribution occurred during a typical 40-min imaging period (Fig. 2*E*); the ratio of control and WMN-treated cells within the follicle and near the follicle edge remained constant. The maintenance of cell distribution over time demonstrates that the aberrant distribution of WMN-treated B cells was not a result of the decrease in velocity slowing their ability to home to the follicle. Furthermore, no significant difference was seen in the instantaneous velocity or localization of wild-type B cells labeled with either CFSE or CMTMR. This agrees with previous studies where it has been demonstrated that velocity changes are not label dependent (19).

WMN treatment disrupts B cell responses to chemokine and the expression of chemokine receptors

Aberrant localization and directional motion of B cells following treatment with WMN prompted us to look for possible disruptions in the chemokine signaling that regulates B cell trafficking to the follicle. To investigate this result, we assessed the ability of the WMN-treated cells to respond to the chemokines relevant to maintaining the B cell follicle, CXCL13, CXCL12, and CCL19, found in the T cell zone. In addition, the effects of brief WMN treatment on B cell migration in response to different chemokines and the surface expression of their cognate receptors were analyzed. The formation and retention of B cells within follicles are regulated by the chemokine CXCL13 acting on CXCR5 receptors (23). B cells

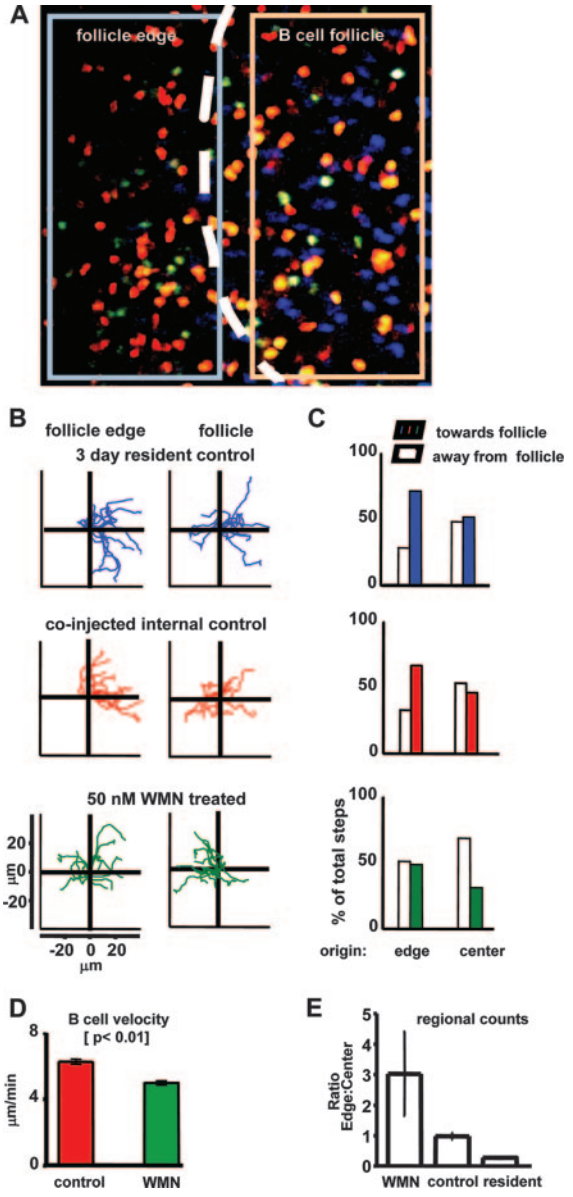

FIGURE 2. Catalytic subunit inhibition alters B cell localization and motility in the lymph node. *A*, Representative image from a triple-label experiment using 3-day resident B cells (blue) to mark the B cell follicle (outlined in white). WMN-treated (50 nM) B cells are labeled green and coinjected control cells are red. Boxed areas represent regions of interest within the B cell follicle or at its edge. The image is a "top view" projection through a 10-μm-thick *z*-slice into the node. *B*, Examples of single cell tracks of 3-day resident (blue), WMN-treated (green), and control (red) B cells whose starting positions lie either at the follicle edge (*left*) or within the follicle (*right*). Each panel shows the superimposed tracks of 12 cells over 7 min with normalized starting coordinates. The follicle boundary runs about vertically as in *A*. *C*, Steps taken by individual cells at an angle toward or away from the follicle were counted in each individual region. Filled bars represent the percentage of total steps taken toward the follicle in each region while the open bars represent the percentage of steps taken away from the follicle in each region ($n > 130$ individual steps for each condition and region). *D*, WMN-treated B cells move with lower average velocity than control B cells. Histograms show means of >1000 instantaneous velocity measurements for control and treated populations ($n = 3$). *E*, WMN-treated B cells are more prevalent at the follicle edge. Histogram shows ratios of the numbers of WMN-treated, control, and 3-day resident B cells found at the follicle edge vs those within the follicle. Data were obtained by averaging cell counts in the two regions as marked in *A* every 5 min during 40 min of imaging time.

[5] The online version of this article contains supplemental material.

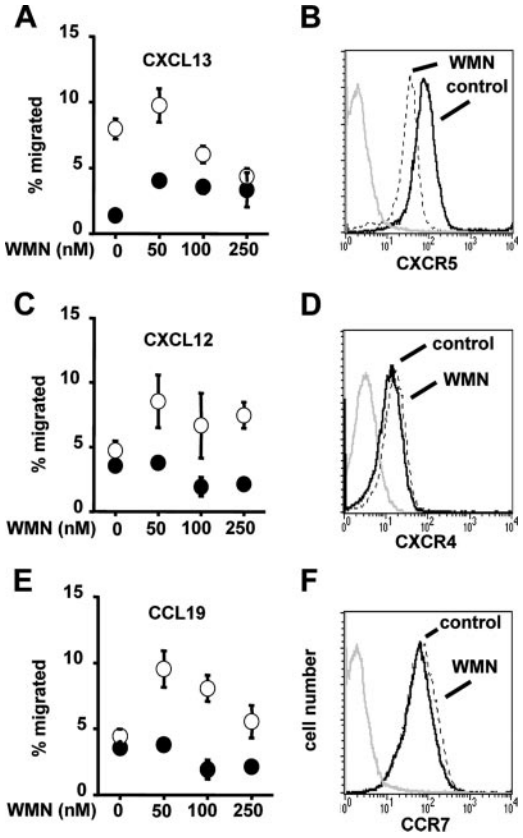

FIGURE 3. Wortmannin treatment alters B cell chemokine response and chemokine receptor expression. *A*, *C*, and *E*, B cell migration measured in a Transwell assay in response to various chemokines after preincubation (15 min) with increasing concentrations of WMN. In each panel, filled symbols represent background levels of migration in the absence of chemokine and open symbols show migration in response to 4 μg/ml CXCL13 (*A*), 0.5 μg/ml CXCL12 (*C*), and 0.5 μg/ml CCL19 (*E*); $n = 3$. *B*, *D*, and *F*, Surface receptor expression of the cognate chemokine receptors, CXCR5 (*B*), CXCR4 (*D*), and CCR7 (*F*), for each Transwell migration assay as determined by FACS analysis in untreated (solid black curves) and WMN-treated B cells (dotted curves, 50 nM for 4 h; solid gray line, isotype control).

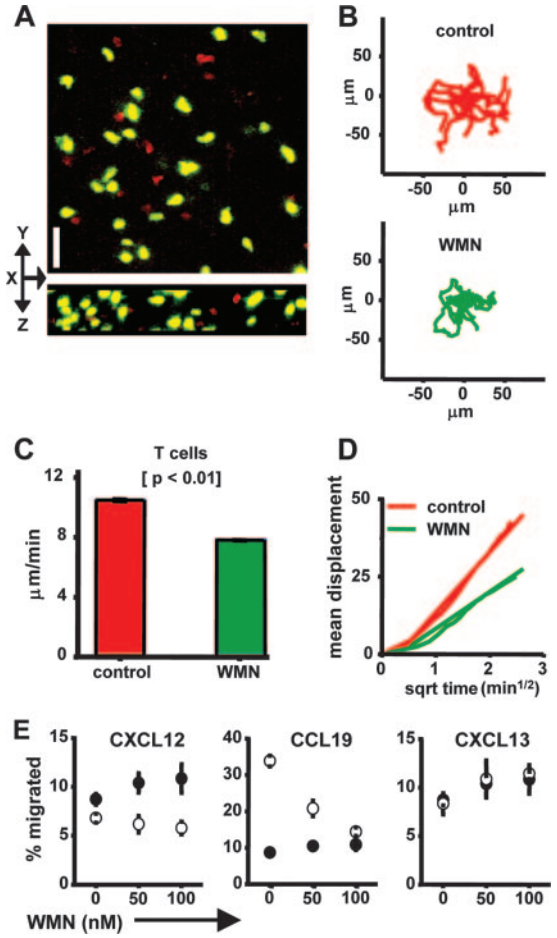

FIGURE 4. Wortmannin treatment reduces T cell velocity but does not affect localization. *A*, T lymphocytes treated with 50 nM WMN (green) colocalize with control lymphocytes (red) (scale bar, 25 μm). *B*, Tracks of control (red) and 50 nM WMN-treated T cells (green) obtained from the same imaging record and with normalized starting coordinates to the origin. *C*, Mean velocities of control (red) and 50 nM WMN-treated T cells derived from >1000 instantaneous velocity measurements. *D*, Plots of mean displacement from origin vs square root of time for control (red) and WMN-treated T cells (green) follow straight lines consistent with random walk motility, ($R^2 = 0.99$; $n = 20$ cells for each group). *E*, Reduction in T cell chemotaxis to CXCL12 and CCL19 after treatment with 50, 100, and 250 nM WMN. T cell migration measured in a Transwell assay in response to chemokines after preincubation (15 min) with increasing concentrations of WMN. In each panel the filled symbols represent background levels of migration in the absence of chemokine and the open symbols show migration in response to 0.5 μg/ml CXCL12, 0.5 μg/ml CCL19, and 4 μg/ml CXCL13.

treated with WMN at concentrations of >50 nM showed strongly decreased migration toward CXCL13 relative to untreated B cells (Fig. 3*A*) and had a reduced surface density of CXCR5 (Fig. 3*B*). We also examined the effects of PI3K catalytic inhibition on chemotaxis directed by CXCL12 and CCL19, chemokines that are typically localized to the paracortex or T cell region. In contrast to the marked effects on CXCL13-driven chemotaxis, control B cells did not show chemotaxis toward CXCL12 and CCL19 but treatment with WMN induced migration toward these chemokines (Fig. 3, *C* and *E*), along with a slight up-regulation in the expression of the cognate CXCR4 and CCR7 receptors (Fig. 3, *D* and *F*). The decrease in B cell responsiveness to CXCL13 and the enhancement of response to CXCL12 and CCL19 are consistent with the altered localization and directed motility of B cells imaged after WMN treatment, reinforcing the conclusion that PI3K catalytic domain activity plays a major role in regulating chemokine responses and receptor expression levels in B cells (7).

PI3K catalytic inhibition reduces T cell velocity but does not affect T cell localization

$CD4^+$ T lymphocytes were imaged within 2 h following adoptive transfer to determine the effect of WMN treatment on their localization and motility within the lymph node. T cells treated with 50 nM WMN (CFSE labeled; green) and control T cells (CMTMR labeled; red) colocalized within the T cell zone (Fig. 4*A* and supplemental video 3). Individual cell tracks of both populations did not reveal an obvious directional preference (Fig. 4*B*), but WMN-treated T cells showed reduced velocities (7.8 μm min^{-1}) relative to coinjected control T cells (10.5 μm min^{-1}; Fig. 4*C*), a reduction of 26%. Both control and treated cells appeared to exhibit random walk motility, as their mean displacements from origin increased roughly as the square root of time (Fig. 4*D*) (19). Motility coefficients derived from the slope of the displacement vs square root time plots yielded a lower value for the WMN-treated T cells (160 vs 240 μm^2 min^{-1} for controls), representing their reduced velocity rather than the altered motility characteristics of the WMN-treated cells. A reduced chemotactic response to CXCL12 and

Table I. *Effects of WMN treatment and PI3K regulatory domain KOs on lymphocyte velocities and morphology*

	Velocity and Shape Changes			
	T Cells		B Cells	
	Velocity Reduction (%)[a]	Shape Index[b]	Velocity Reduction (%)[a]	Shape Index[b]
Control		1.9 ± 0.03		1.6 ± 0.03
Catalytic inhibition				
WMN	26	1.7 ± 0.03[c]	21	1.4 ± 0.03[c]
Regulatory isoform KOs				
p85α	12	1.7 ± 0.03[c]	24	2.1 ± 0.06[c]
p85β	26	1.6 ± 0.03[c]	5	1.5 ± 0.02[d]
p85α and p85β	37	1.4 ± 0.02[c]	Unavailable	

[a] Reduction in cell velocity relative to coinjected internal control population.
[b] Changes in shape index are measured as the cell length divided by the cell width in the *x*–y plane, $n = 262 \pm$ SE.
[c] Paired Student's *t* test; $p < 0.01$ for population shape change relative to control cells.
[d] NS; paired Student's *t* test; $p > 0.05$ for population shape change relative to control cells.

CCL19 was seen after treatment with 50, 100, and 250 nM WMN; T cell migration in response to CXCL13 was identical to that of cells in control wells with no chemokine. These results correlate well with the colocalization of the WMN-treated T cells with the control coinjected T cells (Fig. 4*E*). There were no significant changes in surface chemokine receptor expression in WMN-treated T cells (data not shown). The WMN-treated T cells displayed a consistently less polarized morphology than the coinjected internal control cells as quantified by calculating a "shape index" of cell length divided by cell width (Table I).

p85α KO lymphocytes have reduced velocity and altered B cell morphology

To complement the above studies using a pharmacological approach to assess the role of PI3K catalytic activity in regulating lymphocyte motility and localization in the lymph node, we used KO animals to explore the possible involvement of specific regulatory isoforms of PI3K. Initially, we imaged lymphocytes purified from mice in which disruption of the first exon of *Pik3r1* eliminates the expression of p85α but allows the continued expression of p55α and p50α, the latter of which is expressed abundantly in T cells (3). These p85α KO mice are viable and provided sufficient numbers of T and B cells for adoptive transfer studies. In previous studies it has been shown that B cell proliferation and Ab production are markedly impaired in p85α KO mice, whereas T cell function is apparently normal (1, 3). Class I catalytic functional output is reduced in p85α KO B cells but retained in p85α KO T cells (2, 24).

Simultaneous imaging of cotransferred wild-type (red) and p85α KO T cells (green) demonstrated no change in cell localization. The mean velocity of p85α KO T cells was 12% slower (9.8 μm min^{-1}) than that of coinjected control (wild-type) T cells (11 μm min^{-1}; Fig. 5*A*). The p85α KO T cells displayed an apparent random walk pattern similar to that of the control T cells (Fig. 5*B*), although with a slightly reduced motility coefficient (158 vs 200 μm^2 min^{-1} for controls: Fig. 5*C*) reflecting their slower velocities. The p85α KO T lymphocytes were less polarized than wild-type T cells as determined by shape index analysis (Table I), but they maintained a morphology typical of T cells (Fig. 5*G*).

In contrast to the modest effects of p85α deletion in T cells, striking alterations in cell motility and morphology were seen in B cells. The p85α KO B cells were colocalized with wild-type cells throughout the lymph node but showed a 24% velocity reduction relative to the coinjected internal control cells (4.7 vs 6.2 μm min^{-1}; Fig. 5*D*). Tracks of p85α KO lymphocytes did not reveal any directional preference (Fig. 5*E*) and displayed random walk motility (Fig. 5*F*), although with a reduced motility coefficient (30 vs 61 μm^2 min^{-1} for wild-type B cells). As the p85α KO B cells traversed the B cell follicle they often displayed dramatic alterations in morphology, extending long thin membrane trails at both the leading edge and the trailing edge. Membrane extensions often elongated 20 μm or more from the cell body and facilitated contacts with the coinjected control B cells (red; Fig. 5*H* and supplemental video 4). In contrast, wild-type B cells exhibited small membrane extensions. The striking phenotype of p85α-deficient B cells was evident when compared with coinjected wild-type B cells labeled with either CFSE or CMTMR (data not shown). In contrast to the results seen in WMN-treated B cells, both p85α KO T and B cells were colocalized and evenly distributed in the B cell follicle and T cell zone in the lymph node marked by coinjected wild-type cells.

p85β KO T cells exhibit a larger reduction in motility than B lymphocytes

Class IA p85β is expressed at low levels in both T and B cells, and T cells lacking p85β display unimpaired PI3K signaling output (20). Although this isoform is dispensable for lymphocyte development and proliferation, T cells lacking p85β show reduced apoptosis and increased accumulation following viral infection (1, 2). Interestingly, T lymphocytes lacking p85β demonstrated a significant reduction in mean velocity, moving 26% slower (9.1 μm min^{-1}) than coinjected wild-type control cells (12.2 μm min^{-1}; Fig. 6*A*). p85β KO T cells were distributed evenly among the coinjected internal control population and maintained a random walk pattern similar to that of wild-type cells, although with a reduced motility coefficient (112 vs 255 μm^2 min^{-1}; Fig. 6, *B* and *C*).

In B lymphocytes, deletion of p85β resulted in only modest changes in motility. There was a small (5%), reduction in mean B cell velocity (6.3 vs 6.7 μm min^{-1} for wild-type controls; Fig. 6*D*), accompanied by a very slight reduction in mean displacement of their random tracks and reduction of motility coefficient (62 vs 64 μm^2 min^{-1}; Fig. 6, *E* and *F*). As with other regulatory subunit KO lymphocytes, p85β KO B cells were evenly distributed among the coinjected internal control population.

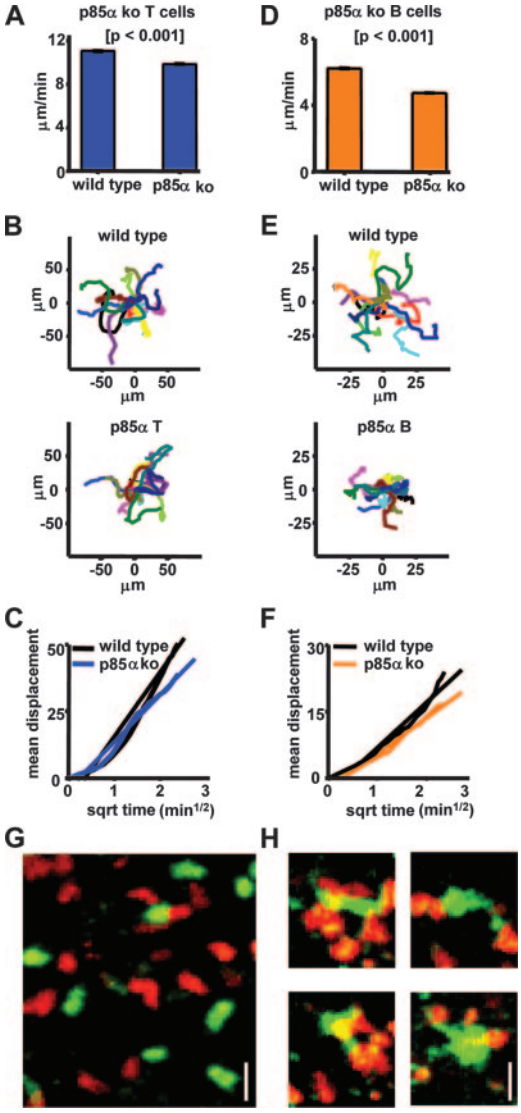

FIGURE 5. Effects of PI3K p85α KO on lymphocyte motility and morphology. *A*, Mean velocity of p85α KO (ko) T cells is slightly reduced as compared with that of wild-type cells. *B*, Representative tracks of wild-type and p85α KO T cells taken from the same imaging record and with normalized starting coordinates. *C*, Mean displacement from origin vs square root (sqrt) time plot for p85α KO T cells (blue) trends toward a straight line (R^2 = 0.98), which is consistent with random walk motility with a slightly reduced motility coefficient as compared with wild-type cells (black; n = 14 cells for each group). *D*, Mean velocity of p85α KO B cells is 24% lower than that of coinjected wild-type B cells. *E*, Representative tracks of wild-type and p85α KO B cells taken from the same imaging record and with normalized starting coordinates. *F*, Mean displacement from origin vs square root time plot for p85α KO B cells (orange) trends toward a straight line (R^2 = 0.98), consistent with random walk motility with a slightly reduced motility coefficient as compared with that of wild-type cells (black; n = 20 cells for each group). *G*, p85α KO T cells (green) show no obvious morphological differences from wild-type T cells (red). *H*, p85α KO B cells (green) exhibit marked morphological abnormalities including dendritic cell-like membrane protrusions and larger cell volume as compared with wild-type B cells (red). Scale bars, 10 μm.

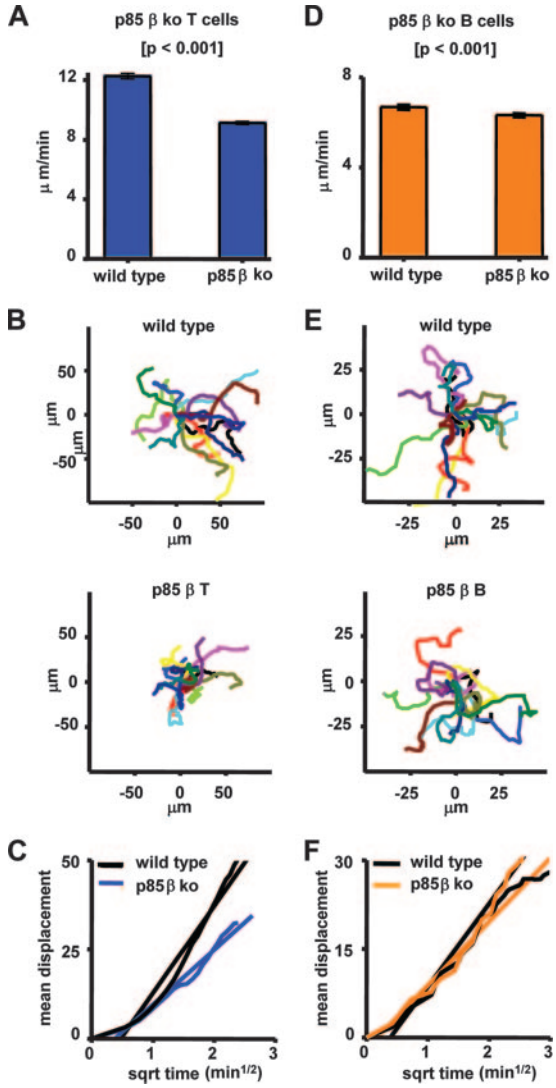

FIGURE 6. PI3K p85β KO lymphocytes. *A*, Mean velocities of wild-type and p85β KO (ko) T cells. *B*, Representative tracks of wild-type and p85β KO T cells taken from the same imaging record and with normalized starting coordinates. *C*, Mean displacement vs square root (sqrt) time plot for p85β KO T lymphocytes (blue) trends toward a straight line (R^2 = 0.98) with a reduced motility coefficient as compared with that of wild-type cells (black). *D–F*, Corresponding data for p85β KO B cells. Mean velocities were derived from >1000 instantaneous measurements; representative tracks are shown for 14 cells and displacement plots are the means of 14 cells.

class IA p85 KO T cells show an additive reduction in T cell velocity

We further examined the involvement of class IA PI3K regulatory isoforms in T cell motility by using a mouse model with more complete ablation of class IA function. In these p85 KO mice, p85β is deleted in all cells (*Pik3r2*-null) and p85α/p55α/p50α are deleted specifically in T cells (*Pik3r1*-flox/Lck-Cre), (2, 3). T cells develop normally but are almost completely devoid of class IA PI3K signaling function (25). These T cells exhibit functional defects including reduced help to B cells and an unexpected tendency to promote the destruction of exocrine glands (25, 26). In two-photon imaging experiments, class IA-deficient T cells showed a 37% decrease in average velocity (7.6 μm/min) relative to internal control cells (12.1 μm min^{-1}; Fig. 7*A* and supplemental video 5). Tracks of double-KO T cells showed no directional preference, but the reduced motility of the cells relative to that of wild-type control cells is readily apparent (Fig. 7*B*), with a reduction in motility coefficient of 46 μm^2/min as compared with 210 μm^2 min^{-1} for the internal control cells (Fig. 7*C*). The class IA-deficient T cells

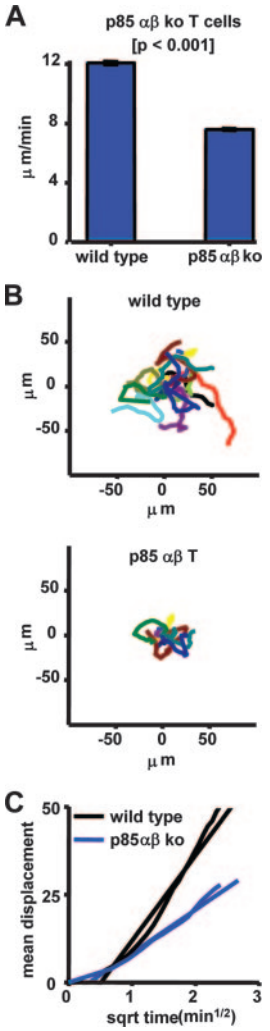

FIGURE 7. PI3K p85$\beta\alpha$/p85β KO lymphocytes *A*, Mean velocities of wild-type and p85α/p85β KO T cells show greater effects on cell motility than those seen in p85α or p85β KO T lymphocytes. *B*, Representative tracks of wild-type and p85α or p85β KO T cells taken from the same imaging record and with normalized starting coordinates. Mean velocities were derived from >1000 instantaneous measurements in each group; representative tracks are shown for 14 cells and displacement plots are the means of 14 cells. *C*, Mean displacement vs square root (sqrt) time plot for p85α or p85β KO T lymphocytes (blue) trends toward a straight line (R^2 = 0.98) with a reduced motility coefficient as compared with wild-type cells (black).

showed a normal distribution within the node, colocalizing with wild-type T cells (Fig. 7*C* and Table I) and with shapes less polarized than those of the control T cells (Table I).

Discussion

Our results demonstrate that basal lymphocyte motility is dependent upon both PI3K enzymatic activity and class IA regulatory subunit function. Through chemical interrogation of the PI3K catalytic subunit, we show that the maintenance of T and B cell velocity in a naive environment is dependent upon PI3K catalytic activity. Furthermore, B cells with inhibited PI3K catalytic subunit activity localize outside of the B cell follicle. Using KO animals, we show that the PI3K class IA regulatory subunits play a cell-type specific role in maintaining basal lymphocyte motility. The predominant class IA PI3K regulatory isoform p85α is necessary to maintain normal T and B cell motility. In addition, B cell morphology is dramatically altered by the loss of the class IA regulatory subunit p85α. Interestingly, the loss of class IA regulatory isoforms produces graded effects on lymphocyte motility. T cells lacking both p85α and p85β exhibit velocity reduction greater in magnitude than cells lacking either subunit alone.

The results we obtained using WMN should be considered in light of other potential targets of this inhibitor. At the concentrations used in our study, WMN effectively blocks the activity of class IA, IB, and III isoforms of PI3K, as well as that of some class II isoforms. It is unlikely that the reduced motility of WMN-treated lymphocytes is due to inhibition of class IB PI3K, because deletion of the sole class IB isoform p110γ has no effect on random motility in vivo (9). Although roles for class II and III isoforms cannot be excluded, these enzymes do not generate the lipid species (PtdIns(3,4,5)P_3) whereas class IA PI3K enzymes do generate PtdIns(3,4,5)P_3, which is known to regulate cell motility in various cell types in vitro and B cell homing in vivo (1, 2, 5, 27). Furthermore, class IA catalytic output is almost completely reduced in T cells lacking p85α/p55α/p50α/p85β, which also demonstrate the most significant decrease in motility (25). To date, there are no other known cellular enzymes with a potential role in motility that are inhibited by WMN at this concentration. Therefore, the effects of wortmannin on basal motility are most likely the result of class IA inhibition. This interpretation, however, does not exclude the participation of regulatory isoforms in a manner distinct from their role in catalytic subunit activation.

WMN treatment of CD43$^-$ B cells perturbed localization, resulting in the displacement of B cells outside of the follicle. Static images of spleen have shown that B cells treated with WMN do not enter the white pulp (7), consistent with our video imaging data showing that B lymphocytes tended to localize at the edge of the lymph node follicle following WMN treatment. Newly transferred untreated B cells were found outside of the follicle and moved with directional preference toward the follicle, presumably homing from the T cell zone into the B cell follicle. This directional preference matched the directional preference of the occasional 3-day resident B cell found outside of the follicle boundary. WMN-treated B lymphocytes originating outside of the follicle boundary did not display a directional preference. Conversely, WMN-treated B cells found inside the follicle moved toward the follicle boundary.

The changes in B cell localization and directional preference are consistent with the changes in B cell chemokine receptor expression and migration after in vitro WMN treatment. B cells treated with WMN in vitro have a lower density of CXCR5, the receptor for CXCL13, a chemokine that plays a role in maintaining the B cell follicle (28, 29). A recent study using Gα_i KO cells demonstrated reduced chemotaxis to CXCL13, illustrating a role for Gα_i signaling in lymphocyte migration (30). This is consistent with studies indicating that Gα_i signaling of certain chemokine receptors may be associated with class IB PI3K signaling (4). CXCL12 is typically found in high concentrations in the T cell zone, and stimulation of its receptor, CXCR4, induces activation of the PI3K/PKB pathway (31). Mature resting B cells lose chemotactic responsiveness to CXCL12 and fail to mobilize intracellular calcium or activate Rac1 or Cdc42 when treated with CXCL12 (32–36). However, when treated with WMN, CD43$^-$ (mature resting) B cells exhibit increased responsiveness to CXCL12, whereas B220$^+$ purified B cells treated with WMN under the same conditions show a significant decrease in responsiveness to CXCL12, consistent with previous studies (data not shown) (7). It is possible that cells isolated by B220 selection contain cell subsets not present in cells isolated by CD43 depletion. WMN inhibition of both catalytic isoforms of PI3K would disrupt class IB signaling

through $G\alpha_i$ and might depress $G\alpha_i$-related migration in chemotactic gradients. However, class IB-deficient B cells were reported to distribute normally in lymph nodes, whereas class IA-deficient (p110δ kinase-dead) B cells were mislocalized (7). We also observed a slight change in the surface expression of CCR7, the receptor for CCL19 and CCL21. It is known that rolling B cells are arrested in the high endothelial venules by both CCR7 (CCL19, CCL21) agonists and by CXCL12 (37). An increased response to CXCL12 as well as to CCL19, combined with a decrease in response to CXCL13, likely contributes both to the enhanced homing of WMN-treated B lymphocytes to peripheral lymph nodes and the localization of these cells at the edge of the B cell follicle. The normal distribution of p85α KO B cells is consistent with the unaltered chemokine receptor expression on these cells and suggests that residual class IA PI3K signaling maintains normal chemokine receptor expression in p85α KO B cells (24).

$CD4^+$ T lymphocytes remained negative for CXCR5 after WMN treatment, and no change in sensitivity to CXCL13 was seen in Transwell assays. Consistent with a previous report, the T cell migration to CXCL12 and CCL19 decreased modestly after WMN treatment (7). Minor changes in CXCL12 and CCL19 responsiveness and no change in CXCL13 response support our observation that WMN-treated T lymphocytes are consistently colocalized with control T lymphocytes. Changes in chemokine receptor surface density were not seen in the class IA PI3K regulatory subunit KO lymphocytes by FACS analysis (data not shown).

Two-photon imaging of lymphocytes lacking various class IA PI3K subunits demonstrates that gene targeting of specific PI3K class IA regulatory subunits alters the motility of T and B lymphocytes to different degrees. p85α KO T lymphocytes have a 12% reduction in velocity, and these cells have a reduced ability to polarize relative to wild-type cells (Table I). The same regulatory isoform KO in B lymphocytes causes a 24% decrease in mean velocity that might be due in part to the altered cell morphology. p85α KO B cells exhibit developmental defects; however all splenic B cell subsets are diminished in p85α KO mice, and the relative frequency of mature follicular B cells is not significantly different from that of wild-type mice (data not shown) (38). The altered morphology of p85α KO B cells might be explained by the contribution of p85α to F-actin formation (17, 39). The regulatory isoform p85α contains a Rac binding domain and has been implicated in a positive feedback loop involving Rac and Cdc42 and F-actin formation at the leading edge of a polarized cell (1). p85β possesses a homologous domain, but the specificity for G protein binding partners might differ. A correlation may exist between morphology changes and Ag responsiveness, because p85α KO T cells retain normal TCR-driven proliferation whereas p85α KO B cells do not proliferate following BCR cross-linking and have a severely reduced ability to produce Abs to T-independent Ags (3, 40).

p85β KO T lymphocytes displayed the greatest reduction in velocity (26%) among lymphocytes lacking a single regulatory subunit. In contrast, p85β KO B lymphocytes had only a slight reduction in velocity (5%). T lymphocytes that are hemizygous for p85β have half the total reduction in velocity of the p85β KO T cells (data not shown), indicating that the effect on cell motility is directly proportional to the expression level of the regulatory subunit. p85β KO T cells retain the ability to offer effective B cell help and demonstrate effective antiviral responses, suggesting that this degree of reduced motility does not compromise these T cell functions (2). p85β KO T cells also persist in lymphoid tissue at late time points following viral infection. Although this phenotype correlates with increased survival during proliferative responses in vitro (2), another possibility is that reduced T cell velocity alters homing and migration patterns during immune response, leading to accumulation in lymphoid organs in these mice.

The effect of knocking out p85α and p85β appears to be additive, with the double-KO T lymphocytes showing a reduction (37%) relative to coinjected internal control cells that is the sum of the reduction in the two single KOs (12% and 26%, respectively). The double-KO T cells are visibly rounded and have a reduced ability to polarize (Table I). Initial characterization of these T cells has shown selective impairments to in vitro stimuli when responses such as calcium flux, proliferation, and cytokine production were measured. Despite the marked defects in motility and biochemical and functional activation, double-KO T cells are able to mediate antiviral immunity and are only partially impaired in their ability to provide help to B cells (26). In addition, p85 null animals develop an autoimmune syndrome with age, characterized by infiltration and destruction of the exocrine glands (26). It is possible that diminished T cell motility in lymphoid and nonlymphoid sites contributes to this phenotype. Further structure-function studies on specific interactions between PI3K regulatory subunits and binding partners may elucidate the molecular basis for altered motility in the absence of regulatory subunits.

WMN-treated T and B lymphocytes accumulated in greater numbers in peripheral lymph nodes than did the coinjected internal control lymphocytes. This finding contrasts with two previous studies reporting either no change or decreased lymph node homing of WMN-treated B cells (7, 16). These differing results could be due to the different time periods of WMN pretreatment and homing analysis among the three studies. We analyzed B cell homing 4 h posttransfer, whereas other investigators used 1.5 and 2 h (7, 16). Delayed homing is consistent with a report that WMN-treated B cells show reduced adhesion and increased rolling in high endothelial venules (16). It is also possible that WMN causes a delay in homing as well as a block in egress once cells enter the lymph node. Lymphocyte egress from lymph nodes is regulated by sphingosine-1-phosphate, the receptor for which is activated by phosphorylation via Akt, a down-stream target of PI3K (41). It is also of interest that sphingosine-1-phosphate has been reported to activate class IB PI3K in other cell types (9, 42).

In summary, class IA PI3K regulatory isoforms play an important functional role in maintaining lymphocyte velocity in the lymph node. It is not yet clear whether the reduced lymphocyte velocities are due to the loss of specific adaptor functions of the regulatory isoforms or to reduced catalytic function. The latter mechanism is supported by reduced T and B lymphocyte velocity when the cells are treated with WMN. However, the reduction in velocity of double-KO T lymphocytes (p85$\alpha\beta$ KO) exceeds the reduction in motility after WMN treatment. In addition, p85α KO B cells have morphological changes not seen in WMN-treated B cells. Lastly, p85β KO T cells have reduced motility without any measurable loss of class IA catalytic output (2). These results indicate specific roles of class IA PI3K regulatory subunits, likely effected by modular domains in these proteins that recruit molecules such as Rac and Cdc42. There is evidence for class IA PI3K adaptor participation upstream or downstream of integrins or their ligands governing motility along tissue superstructures within the lymph node (4, 12–14). A mechanism reliant upon adhesion molecules would suggest that although random motility is characteristic of naive T and B lymphocytes in the lymph node, multiple stimuli may contribute to the forward motility and choice of direction for an individual cell.

Note added in proof. While this paper was under review, another group reported that wortmannin does not alter basal T cell velocity within lymph node tissue (Asperti-Boursin, F., E. Real, G. Bismuth, A. Trautmann, and E. Donnadieu. 2007. CCR7 ligands control basal cell motility within lymph node slices in a phosphoinositide 3-kinase-independent manner. *J. Exp. Med.* 204: 1167–1179). The experimental systems differ in the two reports, and we currently working together to identify possible explanations for the discrepant findings.

Acknowledgments

We thank Amber Donahue, Travis Moore and Jean Oak for excellent assistance with knockout animals as well as Debasish Sen and Sindy Wei for helpful discussion. For technical assistance we thank Dr. Lu Forrest and Dr. Olga Safrina.

Disclosures

The authors have no financial conflict of interest.

References

1. Deane, J. A., and D. A. Fruman. 2004. Phosphoinositide 3-kinase: diverse roles in immune cell activation. *Annu. Rev. Immunol.* 22: 563–598.
2. Deane, J. A., M. J. Trifilo, C. M. Yballe, S. Choi, T. E. Lane, and D. A. Fruman. 2004. Enhanced T cell proliferation in mice lacking the p85β subunit of phosphoinositide 3-kinase. *J. Immunol.* 172: 6615–6625.
3. Suzuki, H., Y. Terauchi, M. Fujiwara, S. Aizawa, Y. Yazaki, T. Kadowaki, and S. Koyasu. 1999. Xid-like immunodeficiency in mice with disruption of the p85α subunit of phosphoinositide 3-kinase. *Science* 283: 390–392.
4. Ward, S. G. 2004. Do phosphoinositide 3-kinases direct lymphocyte navigation? *Trends Immunol.* 25: 67–74.
5. Hannigan, M., L. Zhan, Z. Li, Y. Ai, D. Wu, and C. K. Huang. 2002. Neutrophils lacking phosphoinositide 3-kinase γ show loss of directionality during *N*-formyl-Met-Leu-Phe-induced chemotaxis. *Proc. Natl. Acad. Sci. USA* 99: 3603–3608.
6. Wang, F. 2002. Lipid products of PI(3)Ks maintain persistent cell polarity and directed motility in neutrophils. *Nat. Cell Biol.* 4: 513–518.
7. Reif, K., K. Okkenhaug, T. Sasaki, J. M. Penninger, B. Vanhaesebroeck, and J. G. Cyster. 2004. Cutting edge: differential roles for phosphoinositide 3-kinases, p110γ. and p110δ, in lymphocyte chemotaxis and homing. *J. Immunol.* 173: 2236–2240.
8. Nombela-Arrieta, C., R. A. Lacalle, M. C. Montoya, Y. Kunisaki, D. Megias, M. Marques, A. C. Carrera, S. Manes, Y. Fukui, A. C. Martinez, and J. V. Stein. 2004. Differential requirements for DOCK2 and phosphoinositide-3-kinase γ during T and B lymphocyte homing. *Immunity* 21: 429–441.
9. Nombela-Arrieta, C., T. R. Mempel, S. F. Soriano, I. Mazo, M. P. Wymann, E. Hirsch, A. C. Martinez, Y. Fukui, U. H. von Andrian, and J. V. Stein. 2007. A central role for DOCK2 during interstitial lymphocyte motility and sphingosine-1-phosphate-mediated egress. *J. Exp. Med.* 204: 497–510.
10. Huang, Y. E., M. Iijima, C. A. Parent, S. Funamoto, R. A. Firtel, and P. Devreotes. 2003. Receptor-mediated regulation of PI3Ks confines PI(3,4,5)P3 to the leading edge of chemotaxing cells. *Mol. Biol. Cell* 14: 1913–1922.
11. Curnock, A. P., Y. Sotsios, K. L. Wright, and S. G. Ward. 2003. Optimal chemotactic responses of leukemic T cells to stromal cell-derived factor-1 requires the activation of both class IA and IB phosphoinositide 3-kinases. *J. Immunol.* 170: 4021–4030.
12. Sano, M., A. R. Leff, S. Myou, E. Boetticher, A. Y. Meliton, J. Learoyd, A. T. Lambertino, N. M. Munoz, and X. Zhu. 2005. Regulation of interleukin-5-induced β_2-integrin adhesion of human eosinophils by phosphoinositide 3-kinase. *Am. J. Respir. Cell Mol. Biol.* 33: 65–70.
13. Munugalavadla, V., J. Borneo, D. A. Ingram, and R. Kapur. 2005. p85α subunit of class IA PI-3 kinase is crucial for macrophage growth and migration. *Blood* 106: 103–109.
14. Perez, O. D., S. Kinoshita, Y. Hitoshi, D. G. Payan, T. Kitamura, G. P. Nolan, and J. B. Lorens. 2002. Activation of the PKB/AKT pathway by ICAM-2. *Immunity* 16: 51–65.
15. Khwaja, A., K. Lehmann, B. M. Marte, and J. Downward. 1998. Phosphoinositide 3-kinase induces scattering and tubulogenesis in epithelial cells through a novel pathway. *J. Biol. Chem.* 273: 18793–18801.
16. Ortolano, S., I. Y. Hwang, S. B. Han, and J. H. Kehrl. 2006. Roles for phosphoinositide 3-kinases, Bruton's tyrosine kinase, and Jun kinases in B lymphocyte chemotaxis and homing. *Eur. J. Immunol.* 36: 1285–1295.
17. Jimenez, C., R. A. Portela, M. Mellado, J. M. Rodriguez-Frade, J. Collard, A. Serrano, A. C. Martinez, J. Avila, and A. C. Carrera. 2000. Role of the PI3K regulatory subunit in the control of actin organization and cell migration. *J. Cell Biol.* 151: 249–262.
18. Nguyen, Q. T., N. Callamaras, C. Hsieh, and I. Parker. 2001. Construction of a two-photon microscope for video-rate Ca^{2+} imaging. *Cell Calcium* 30: 389–393.
19. Miller, M. J., S. H. Wei, I. Parker, and M. D. Cahalan. 2002. Two-photon imaging of lymphocyte motility and antigen response in intact lymph node. *Science* 296: 1869–1873.
20. Fruman, D. A., F. Mauvais-Jarvis, D. A. Pollard, C. M. Yballe, D. Brazil, R. T. Bronson, C. R. Kahn, and L. C. Cantley. 2000. Hypoglycaemia, liver necrosis and perinatal death in mice lacking all isoforms of phosphoinositide 3-kinase p85 α. *Nat. Genet.* 26: 379–382.
21. Brachmann, S. M., C. M. Yballe, M. Innocenti, J. A. Deane, D. A. Fruman, S. M. Thomas, and L. C. Cantley. 2005. Role of phosphoinositide 3-kinase regulatory isoforms in development and actin rearrangement. *Mol. Cell. Biol.* 25: 2593–2606.
22. Orban, P. C., D. Chui, and J. D. Marth. 1992. Tissue- and site-specific DNA recombination in transgenic mice. *Proc. Natl. Acad. Sci. USA* 89: 6861–6865.
23. Cyster, J. G., V. N. Ngo, E. H. Ekland, M. D. Gunn, J. D. Sedgwick, and K. M. Ansel. 1999. Chemokines and B-cell homing to follicles. *Curr. Top. Microbiol. Immunol.* 246: 87–92; discussion 93.
24. Hess, K. L., A. C. Donahue, K. L. Ng, T. I. Moore, J. Oak, and D. A. Fruman. 2004. Frontline: The p85α isoform of phosphoinositide 3-kinase is essential for a subset of B cell receptor-initiated signaling responses. *Eur. J. Immunol.* 34: 2968–2976.
25. Deane, J. A., M. G. Kharas, J. S. Oak, L. N. Stiles, J. Luo, T. I. Moore, H. Ji, C. Rommel, L. C. Cantley, T. E. Lane, and D. A. Fruman. 2007. T cell function is partially maintained in the absence of class IA phosphoinositide 3-kinase signaling. *Blood* 109: 2894–2902.
26. Oak, J. S., J. A. Deane, M. G. Kharas, J. Luo, T. E. Lane, L. C. Cantley, and D. A. Fruman. 2006. Sjogren's syndrome-like disease in mice with T cells lacking class 1A phosphoinositide-3-kinase. *Proc. Natl. Acad. Sci. USA* 103: 16882–16887.
27. Vanhaesebroeck, B., G. E. Jones, W. E. Allen, D. Zicha, R. Hooshmand-Rad, C. Sawyer, C. Wells, M. D. Waterfield, and A. J. Ridley. 1999. Distinct PI(3)Ks mediate mitogenic signalling and cell migration in macrophages. *Nat. Cell. Biol.* 1: 69–71.
28. Reif, K., E. H. Ekland, L. Ohl, H. Nakano, M. Lipp, R. Forster, and J. G. Cyster. 2002. Balanced responsiveness to chemoattractants from adjacent zones determines B-cell position. *Nature* 416: 94–99.
29. Ansel, K. M., R. B. Harris, and J. G. Cyster. 2002. CXCL13 is required for B1 cell homing, natural antibody production, and body cavity immunity. *Immunity* 16: 67–76.
30. Han, S. B., C. Moratz, N. N. Huang, B. Kelsall, H. Cho, C. S. Shi, O. Schwartz, and J. H. Kehrl. 2005. Rgs1 and Gnai2 regulate the entrance of B lymphocytes into lymph nodes and B cell motility within lymph node follicles. *Immunity* 22: 343–354.
31. Tilton, B., L. Ho, E. Oberlin, P. Loetscher, F. Baleux, I. Clark-Lewis, and M. Thelen. 2000. Signal transduction by CXC chemokine receptor 4. Stromal cell-derived factor 1 stimulates prolonged protein kinase B and extracellular signal-regulated kinase 2 activation in T lymphocytes. *J. Exp. Med.* 192: 313–324.
32. Honczarenko, M., R. S. Douglas, C. Mathias, B. Lee, M. Z. Ratajczak, and L. E. Silberstein. 1999. SDF-1 responsiveness does not correlate with CXCR4 expression levels of developing human bone marrow B cells. *Blood* 94: 2990–2998.
33. D'Apuzzo, M., A. Rolink, M. Loetscher, J. A. Hoxie, I. Clark-Lewis, F. Melchers, M. Baggiolini, and B. Moser. 1997. The chemokine SDF-1, stromal cell-derived factor 1, attracts early stage B cell precursors via the chemokine receptor CXCR4. *Eur. J. Immunol.* 27: 1788–1793.
34. Yamamoto, D., Y. Sonoda, M. Hasegawa, M. Funakoshi-Tago, E. Aizu-Yokota, and T. Kasahara. 2003. FAK overexpression upregulates cyclin D3 and enhances cell proliferation via the PKC and PI3-kinase-Akt pathways. *Cell. Signal.* 15: 575–583.
35. Zhang, S., and H. E. Broxmeyer. 1999. p85 subunit of PI3 kinase does not bind to human Flt3 receptor, but associates with SHP2, SHIP, and a tyrosine-phosphorylated 100-kDa protein in Flt3 ligand-stimulated hematopoietic cells. *Biochem. Biophys. Res. Commun.* 254: 440–445.
36. Fedyk, E. R., D. H. Ryyan, I. Ritterman, and T. A. Springer. 1999. Maturation decreases responsiveness of human bone marrow B lineage cells to stromal-derived factor 1 (SDF-1) *J. Leukocyte Biol.* 66: 667–673.
37. von Andrian, U. H., and T. R. Mempel. 2003. Homing and cellular traffic in lymph nodes. *Nat. Rev. Immunol.* 3: 867–878.
38. Donahue, A. C., K. L. Hess, K. L. Ng, and D. A. Fruman. 2004. Altered splenic B cell subset development in mice lacking phosphoinositide 3-kinase p85α. *Int. Immunol.* 16: 1789–1798.
39. Welch, H. C., W. J. Coadwell, L. R. Stephens, and P. T. Hawkins. 2003. Phosphoinositide 3-kinase-dependent activation of Rac. *FEBS Lett.* 546: 93–97.
40. Fruman, D. A., S. B. Snapper, C. M. Yballe, L. Davidson, J. Y. Yu, F. W. Alt, and L. C. Cantley. 1999. Impaired B cell development and proliferation in absence of phosphoinositide 3-kinase p85α. *Science* 283: 393–397.
41. Lee, M. J., S. Thangada, J. H. Paik, G. P. Sapkota, N. Ancellin, S. S. Chae, M. Wu, M. Morales-Ruiz, W. C. Sessa, D. R. Alessi, and T. Hla. 2001. Akt-mediated phosphorylation of the G protein-coupled receptor EDG-1 is required for endothelial cell chemotaxis. *Mol. Cell* 8: 693–704.
42. Igarashi, J., and T. Michel. 2001. Sphingosine 1-phosphate and isoform-specific activation of phosphoinositide 3-kinase β. Evidence for divergence and convergence of receptor-regulated endothelial nitric-oxide synthase signaling pathways. *J. Biol. Chem.* 276: 36281–36288.